Received: 14 June 2022 | Revised: 9 August 2022 | Accepted: 10 August 2022

DOI: 10.1111/jmi.13139

Journal of Microscopy RMS

THEMED ISSUE PAPER

# intER-ACTINg: The structure and dynamics of ER and actin are interlinked

**Charlotte Pain**[1] | **Frances Tolmie**[1] | **Stefan Wojcik**[1] | **Pengwei Wang**[2] | **Verena Kriechbaumer**[1]

[1]Plant Cell Biology, Department of Biological and Medical Sciences, Oxford Brookes University, Oxford, UK

[2]Key Laboratory of Horticultural Plant Biology (Ministry of Education), College of Horticulture and Forestry Science, Huazhong Agricultural University, Wuhan, China

**Correspondence**
Verena Kriechbaumer, Plant Cell Biology, Department of Biological and Medical Sciences, Oxford Brookes University, Oxford OX3 0BP, UK.
Email: vkriechbaumer@brookes.ac.uk

**Abstract**

The actin cytoskeleton is the driver of gross ER remodelling and the movement and positioning of other membrane-bound organelles such as Golgi bodies. Rapid ER membrane remodelling is a feature of most plant cells and is important for normal cellular processes, including targeted secretion, immunity and signalling. Modifications to the actin cytoskeleton through pharmacological agents such as Latrunculin B and phalloidin, or disruption of normal myosin function also affect ER structure and/or dynamics. Here, we investigate the impact of changes in the actin cytoskeleton on structure and dynamics on the ER as well as in return the impact of modified ER structure on the architecture of the actin cytoskeleton. By expressing actin markers that affect actin dynamics, or expressing of ER-shaping proteins that influence ER architecture, we found that the structure of ER-actin networks is closely inter-related; affecting one component is likely to have a direct effect on the other. Therefore, our results indicate that a complicated regulatory machinery and cross-talk between these two structures must exist in plants to co-ordinate the function of ER-actin network during multiple subcellular processes. In addition, when considering organelle structure and dynamics, the choice of actin marker is essential in preventing off-target organelle structure and dynamics modifications.

KEYWORDS
actin, actin marker, ActinCb, endoplasmic reticulum, FABD2, Lifeact, structure analysis

## 1 | INTRODUCTION

### 1.1 | The importance of the ER and actin cytoskeleton in normal cellular functioning

The endoplasmic reticulum (ER) and actin cytoskeleton are both essential for normal cellular functioning, and function in concert across a diverse suite of cellular processes. The ER is primarily responsible for the synthesis, packaging and quality control of critical cellular components[1] and functions in the production of components of plant cell immunity,[2] efficient metabolism of plant hormones such as ethylene[3–5] and recruitment of actin regulatory complexes such as the WAVE/SCAR complex.[6] Due to the pervasiveness of ER throughout the cytoplasm, the ER also acts as an essential reservoir of cell

signalling components such as calcium,[7] and during seed development holds key seed storage proteins including globulins and prolamins.[8] The actin cytoskeleton, through the action of actin-binding proteins which physically link actin filaments to a variety of cellular constituents,[10,9] is required for cellular processes such as cell division and elongation,[11] endocytosis and vesicle trafficking[13,14,12,15] and immunity.[17–19,16]

The structure of the ER, and the varying proportions of the structural ER subdomains (tubules and cisternae), may play a role in the normal functioning of the ER. A high abundance of cisternae has been associated with increased production of secretory proteins, based on evidence of an increased proportion of cisternae being commonly associated with cells with increased secretory demands in both plants and animals.[21,20,22] The structure of the plant ER is maintained by members of at least three protein families: the reticulon protein family, responsible for inducing tubules and membrane curvature,[25,23,24] the Lunapark protein family, essential in cisternae formation[26] and RHD3, a putative plant ER fusogen.[28,29,27] Alongside ER shaping proteins, both microtubules and the actin cytoskeleton play some role in maintaining the structure of the ER. The ER is anchored onto the microtubule network, which plays a role in stabilising ER junctions and tubule dead-ends,[32,30,31] while slow tubule extensions are thought to also be mediated by microtubules.[31] In mammalian cells, the structure of the ER in lamellipodia is closely aligned to that of the underlying microtubules and depolymerisation of microtubules causes some of the ER to coalesce into cisternae.[33] Furthermore, recent super-resolution studies have shown that microtubules play an essential role in supporting previously not visible nano-structures within ER cisternae.[34]

Just as the structure of the ER is essential for normal ER function, it is also thought that the architecture of the actin cytoskeleton is essential for some cellular functions. Specific actin filament conformations are required for cell elongation and expansion, including root hair development, pollen tube growth, pavement cell morphogenesis and trichome development.[37,36,35] Moreover, the actin cytoskeleton must be able to remodel with correct orientation and structural organisation to ensure appropriate, directed vesicle traffic, for example during the development of ingrowth papillae in the transfer cells of *Vicia faba*.[38]

## 1.2 | The interconnectivity of the actin and the ER

The ER in the majority of plant cells is in a constant state of flux, remodelling at a rapid rate for reasons that have not yet been fully elucidated.[39] This remodelling is achieved through ER tubule extension, retraction and sliding, alongside cisternae formation, collapse, transmutation and translocation.[42,41,39,40] Bulk translocation of the ER also occurs in streams, found at variable depths within the cell, which can reach speeds of up to 10 $\mu$m/s, similar to the rate of movement of other organelles.[41,43]

The remodelling of the ER is mostly driven by the underlying actin cytoskeleton, working in concert with ER-actin bridging proteins (e.g. SYP73, NET3B) and myosin motors,[44,45] in particular class XI myosins. Disruption of the class XI myosins, through over-expression of truncated myosin XI tail fusions that act in a dominant-negative manner, or genetically knocking-out the expression of certain myosin genes, perturbs both the structure and the dynamics of the ER.[48,47,46,43] Similar, but more extreme perturbations are also seen on depolymerisation of the filamentous actin cytoskeleton through treatment with Latrunculin B (Lat B), a drug that prevents repolymerisation of actin filaments.[49] Treatment with Lat B almost entirely abolishes ER movement, save for residual oscillations along tubules and cisternae edges, and the structure of the ER is perturbed.[44,50] Furthermore, the actin cytoskeleton is particularly involved in the extension of ER tubules,[51] though the existence of tubules themselves are controlled by internal ER factors.[52] The movement of other organelles, such as the Golgi bodies, are also heavily dependent on the function of the actin cytoskeleton.[53,54]

## 1.3 | Visualising the actin cytoskeleton

Common cellular compartment labelling techniques, such as the use of direct antibody labelling and fluorescent tagging of proteins of interest, are not easily applicable to the actin cytoskeleton. One of the primary challenges of fluorescent labelling of the actin cytoskeleton is that actin exists as two pools within cells – monomeric actin (G-actin) and filamentous actin (F-actin), with F-actin primarily responsible for cellular organisation and dynamics.[55] Labelling of actin directly results in a large pool of the monomeric actin becoming dominant, producing a high background interference when collecting images.[56] It has also been reported that chimeric actin with a large fluorescent tag, is not as efficiently incorporated into actin filaments as untagged actin.[56] Though much smaller chemical fluorophores exist, they are technically challenging to work with.[56] Instead, the majority of actin imaging is performed by fluorescently tagging either entire, or just the active subdomains of actin binding proteins. Two commonly used actin binding protein subdomains are FABD2 and Lifeact, the C-terminal half of the Arabidopsis fimbrin 1 protein and the first 17 amino

acids of the *Saccharomyces cerevisiae* actin binding protein Abp140, respectively.[58,57,60,59,61] A more recent development has been the actin chromobody, a 13 kDa actin binding alpaca chromobody (ActinCb) which has been used effectively for live cell actin imaging by confocal microscopy.[62,45]

Prior work comparing the differences between FABD2 and Lifeact by van der Honing et al.[63] reveals differences in the apparent architecture and the rate of actin filament movement.[59,61,63] Furthermore, both Lifeact and actin chromobody expression in tobacco leaf epidermal cells have been shown to reduce the movement of Golgi bodies, yet the meandering index of Golgi bodies (the ratio of the displacement to velocity) is not affected by over-expression of the actin chromobody.[62] This is suggestive that though the rate of Golgi body movement is reduced, the Golgi bodies are moving in a similar way.

Despite the ubiquitous use of a variety of actin markers, little is known about the effect of actin visualisation on the closely connected, overlying ER. Furthermore, the effect of modifications to the ER on the architecture of the underlying actin cytoskeleton has not been fully investigated. Here we attempt to understand the interconnectivity of actin cytoskeleton and ER structure.

## 2 | RESULTS

### 2.1 | The impact of transient over-expression of actin markers on organelle structure and dynamics

Visualisation of the actin cytoskeleton in living plant cells usually requires the attachment of actin-binding proteins fused to fluorescent proteins to actin filaments, as dyes such as phalloidin, require cell fixation or, in the case of rhodamine-phalloidin staining favour actin bundles as opposed to the entirety of the actin network.[64] Actin markers like FABD2, Lifeact and an actin chromobody (ActinCb; Figure 1) are most commonly imaged using confocal microscopy. Though all three probes localise to the actin cytoskeleton, the structure of the cytoskeleton varies in response to the actin probe used. To enable reliable studies on the interaction between ER and actin or even on the actin cytoskeleton alone, it is crucial to investigate if labelling of the actin cytoskeleton affects its functionality for example in regards to the interplay with the ER.

To assess in detail whether the structure and dynamics of the plant ER is affected by the over-expression of actin markers, the ER of tobacco leaf epidermal cells was analysed using AnalyzER.[41] Full details of the variables calculated by AnalyzER, and how they are calculated, are detailed in Table S1. The ER was visualised each time using transient expression of the ER lumenal marker RFP-HDEL, transiently co-expressed alongside either ST-GFP (Figure 2Ai–iii, the Golgi body marker ST-GFP is used to act as a dual infiltration control), ST-GFP after treatment with Latrunculin B (Figure 2Aiv–vi, a pharmacological agent that prevents repolymerisation of the actin cytoskeleton), YFP-ActinCb (Figure 2Avii–ix), GFP-Lifeact (Figure 2Ax–xii) or GFP-FABD2 (2Axiii–xv). A significant difference between all groups was identified by MANOVA (Pillai's trace, $p$-value $= 2.63 \times 10^{-20}$ and Roy's largest root, $p$-value $= 1.44 \times 10^{-17}$). To visualise how the structure and dynamics of the ER is changed by expression of actin probes and treatment with Lat B, the first 4 discriminate canonical variables were plotted pairwise. Though separation between the different treatment groups was not complete, this is not surprising as basic ER structure is required for normal cell functioning and extreme modifications to ER structure most likely result in cell death. The first and second canonical variables appeared to partially separate ER structure variable changes on Lat B treatment and on GFP-FABD2 over-expression (Figure 2B). The third canonical variable appeared to separate GFP-Lifeact from other treatment groups (Figure 2C), while the separation on the fourth canonical variable was less clear (Figure 2D). A dendrogram plot comparing the group means after the ANOVA revealed that both GFP-Lifeact and YFP-ActinCb cause similar changes in ER structure (Figure 2E). GFP-FABD2 over-expression formed a different clade, and Lat B treatment results in even more extreme changes in ER structure.

After confirmation that there was a significant difference between the ER structure variables measured after over-expression of actin markers and treatment with Lat B, we proceeded to use multiple ANOVA's (with a Bonferroni correction for multiple comparisons applied to adjust each $p$-value) to assess which ER variables are modified by over-expression of actin markers or drug treatments (Table S2). Significant changes in global speed, maximum speed and persistency of both tubules and cisternae were detected. While cisternae showed a modified geometry, polygonal regions showed a modified geometry and area. Very little change in the distribution of fluorophores through the lumen of cisternae was identified in the presence of actin markers measured through texture image analysis techniques (see Section 4 for more details).

To further contextualise the results, the percentage change for each variable has been included (Table 1). GFP-FABD2 appeared to significantly affect ER dynamics, reducing mean tubule speed by 42.6% and mean cisternae speed by 51.5%. The impact of GFP-FABD2 on ER dynamics was even more extreme than the impact of treatment with Lat B, which reduced mean tubule and cisternal speed by 31.4% and 48.2%, respectively. In addition, the ER became

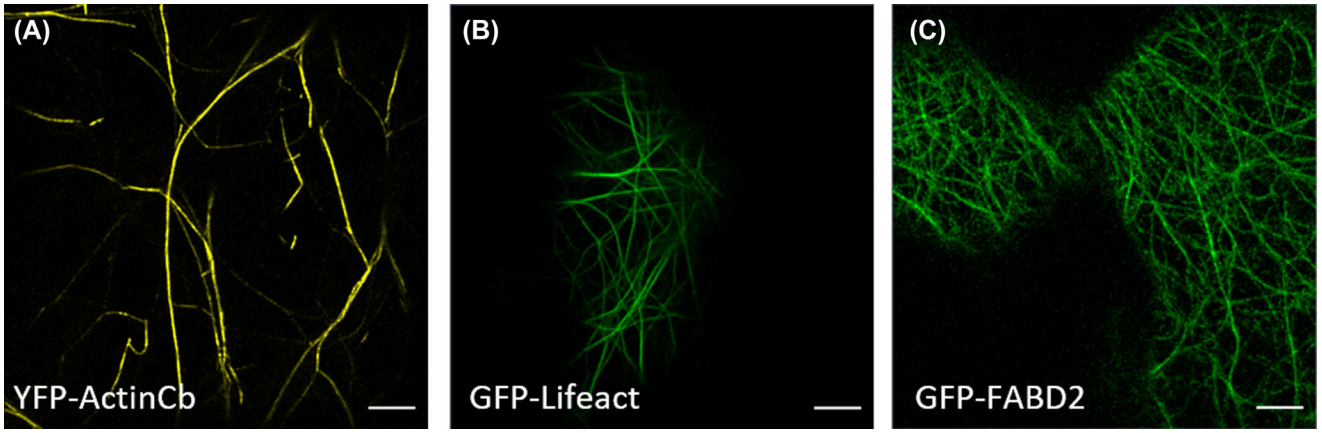


**FIGURE 1** Labelling of the actin cytoskeleton with different fluorescent marker constructs. Representative images of tobacco leaf epidermal cells with comparable expression of the actin markers (A) YFP-ActinCb, (B) GFP-Lifeact and (C) GFP-FABD2 using confocal microscopy. Scale bars = 5 $\mu$m

**TABLE 1** Mean percentage change in measured ER structure and dynamic metrics

| ER structural subdomain | Variable | Lat B | YFP-ActinCb | GFP-Lifeact | GFP-FABD2 |
|---|---|---|---|---|---|
| **Tubules** | Global speed | −31.4%** | +22.2%* | −13.6% | −42.6%*** |
| | Maximum speed | −26.0%* | +18.9% | −10.7% | −35.1%*** |
| | Mean persistency | +32.5%* | +29.1% | +13.5% | +64.8%*** |
| **Cisternae** | Area | +14.3%* | +18.9% | +20.5% | −22.7% |
| | Elongation | −5.7%* | −3.9%* | −5.4%** | −6.5%*** |
| | Global speed | −48.2%** | −31.3%* | −22.3% | −51.5%*** |
| | Maximum speed | −24.2% | −18.6% | −11.9% | −36.2%*** |
| | Mean persistency | +31.3%*** | +12.7% | +6.0% | +32.1%*** |
| **Polygonal region** | Area | +69.7% | +10.3% | +14.1% | +48.1%** |
| | Circularity | +3.1% | −0.6% | −2.8% | −2.9%* |
| | Roughness | −4.0% | −0.3% | +2.9% | +1.6% |
| | Elongation | −5.8%** | −3.3% | +0.3% | −4.2%* |

*Note*: The mean percentage change in ER structure metrics after treatment with Lat B or co-expression with three actin markers: GFP-FABD2, GFP-Lifeact and YFP-ActinCb. Comparisons are all given against the control ER structure. Only ER metrics that show a significant change after ANOVA analysis (Table S2) are included. Significant changes in the in ER structure and dynamics after applying a post hoc Tukey's HSD (with Bonferroni correction applied to all *p*-values) are denoted using asterisks.

*$p$-value ≤ 0.05,

**$p$-value ≤ 0.01

***$p$-value ≤ 0.001.

more 'widely spaced' on GFP-FABD2 over-expression, with the mean polygonal region size increased by 48.1%. These increased gaps in the ER network may affect the distribution of other organelles such as Golgi bodies that are in direct contact with the ER. Organelle position and dynamics, including that of the ER itself, have been correlated with plant responses to pathogen attack, wounding and heavy metal toxicity.[66,67,65] Therefore, it is a concern that the over-expression of GFP-FABD2 may inhibit plant responses to these stressors. Some aspects of this phenotype, such as the reduced speed of ER remodelling, are reminiscent of ER structure and dynamic changes that occur on over-expression of the XI-K tail domains, which functions in a dominant-negative manner.[68,48,46] Hence, an alternative explanation may be that GFP-FABD2 over-expression affects the functionality of myosins. YFP-ActinCb and GFP-Lifeact over-expression appeared to significantly alter fewer ER structural metrics and to a lesser extent; with less extreme and largely non-significant reductions in ER dynamics. Polygonal regions seem largely

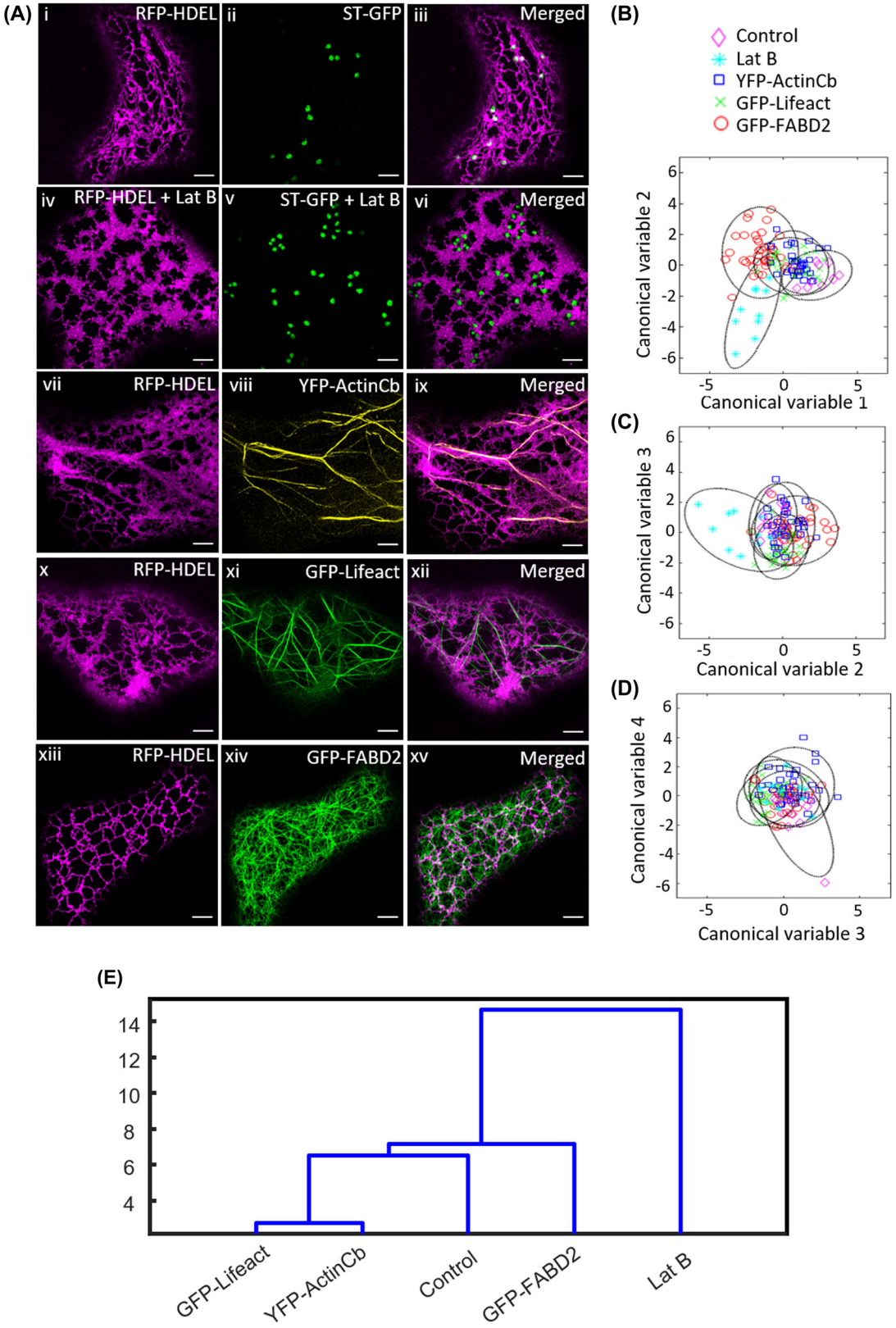


**FIGURE 2** ER structure is modified by over-expression of the actin markers YFP-ActinCb, GFP-Lifeact and GFP-FABD2. (A) Transient over-expression of the ER lumenal marker RFP-HDEL (magenta), infiltrated alongside either a second control construct or one of three actin markers (green or yellow). Example images shown for (i–iii) RFP-HDEL and the Golgi body marker ST-GFP; (iv–vi) RFP-HDEL and ST-GFP after treatment with Latrunculin B; (vii–ix) RFP-HDEL and YFP-ActinCb; (x–xii) RFP-HDEL and GFP-Lifeact; (xii–xv) RFP-HDEL and GFP-FABD2. Separation of different treatments produced using the (B) first and second, (C) second and third and (D) third and fourth discriminatory canonical variables. The 95% confidence level is shown by the black dotted line. (E) A cluster dendrogram of the group means. Time series for clustering results obtained over five biological repeats, with a total of 129 time-series of cells analysed. Scale bars = 5 $\mu$m

unaffected but cisternae were slightly less elongated on YFP-ActinCb and GFP-Lifeact over-expression (−3.9% and −5.4%, respectively).

Alongside affecting ER structure, the distribution of Golgi bodies throughout the cell was also affected. Compared to control, there were significant changes in the distribution of Golgi bodies on treatment with Lat B to depolymerise the actin cytoskeleton, and on co-expression of YFP-ActinCb, and GFP-FABD2 (Figure S1). Interestingly, over-expression of GFP-Lifeact appeared to have no significant impact on the distribution of Golgi bodies.

Actin markers are frequently infiltrated into tobacco leaf epidermal cells as part of transient expression experiments. In these experiments, the level of expression is often approximately controlled for by varying the optical density of the infiltration medium used, thus delivering more or less agrobacteria in the same volume of infiltration buffer. A commonly used infiltration $OD_{600}$ is 0.1. When expressing GFP-FABD2 at commonly used level, fragmentation of the ER, whereby the ER is broken up into numerous distinct regions, occurred in approximately 25% of cells (Figure 3A and B). This was irrespective of the concentration (ranging from $OD_{600}$ 0.01–0.1) of the agrobacterium media used, however did not occur on expression of either GFP-Lifeact or YFP-ActinCb (Figure 3C). Fragmentation of the ER is likely to have serious consequences for ER function, particularly in terms of the transport of lumenal contents through the ER, such as $Ca^{2+}$.[69]

## 2.2 | The impact of stable actin marker expression on ER structure in Arabidopsis

The effect of stable expression of actin markers on ER structure in Arabidopsis seedlings was also investigated. Stable expression lines for GFP-ActinCb, GFP-Lifeact[61] and GFP-FABD2,[63] respectively, were stained with the lipid dye Rhodamine B and imaged using confocal microscopy (Figure 4A–D). The structure of the ER was analysed using the AnalyzER software as described previously. Significant differences in ER tubule length, and polygonal region area, circularity and roughness were identified by ANOVA ($p$-values $1.62 \times 10^{-2}$, $4.31 \times 10^{-2}$, $1.73 \times 10^{-2}$ and $1.73 \times 10^{-2}$, respectively, with all $p$-values corrected for multiple comparisons using the Bonferroni correction; Table S3). Comparison of the mean percentage change in ER structural characteristics revealed that GFP-FABD2 over-expression induced the largest changes, increasing tubule length by 25% and polygonal region area by 61.5% (Table 2). However, the only statistically significant change identified by Tukey's HSD with Bonferroni correction, was a significant reduction in polygonal region circularity (6.1%, $p$-value $3.82 \times 10^{-2}$) and a significant increase in polygonal region roughness (5.8%, $p$-value $3.82 \times 10^{-2}$). In conclusion, stable expression of GFP-ActinCb and GFP-Lifeact did not appear to affect ER structure, however, Arabidopsis lines stably expressing GFP-FABD2 showed a perturbed ER structure, which may in turn affect the functional responses of these Arabidopsis lines.

## 2.3 | The structure of the ER affects the underlying cytoskeleton architecture

To investigate whether the structure of the ER affects the architecture of the underlying actin cytoskeleton, the actin marker YFP-ActinCb was co-expressed with the ER membrane marker CXN-mCherry (Figure 5A)[23] and known ER structure-modifying proteins RFP-LNP1 (Figure S6B) and RFP-LNP2 (Figure S6C), both of which induce cisternae,[26] and RFP-RTN1, which increases the proportion of tubules within the ER upon over-expression (Figure S6D).[23]

When using YFP-ActinCb as an actin marker, RFP-LNP1 over-expression resulted in a significant increase in the density of actin filaments, which appeared to be particularly dense under the induced cisternae (Figure 5). While not statistically significant, there was also an increase in density of actin filaments on RFP-LNP2 over-expression. In addition, there was a decrease in the density of actin filaments on RFP-RTN1 over-expression, though again it was not statistically significant (Table S4). This may indicate that the density of actin filaments is dependent on the overlying ER architecture. Actin filaments have been shown to support fenestrae (small holes) in liver sinusoidal endothelial cell (LSEC) membranes.[70] ER cisternae of mammalian cells have recently been described as regions containing many of these subresolution holes, though thus far only the microtubule cytoskeleton has been implicated in the distribution and dynamics of these holes.[72,71,34] Therefore, the apparent increase in actin density under induced ER cisternae may be linked to a requirement for dense filament networks to support the complex, fenestrated structure of the overlying cisternae. As filament density was increased, actin filament bundling was significantly decreased on stable over-expression of RFP-LNP1 and 2. Both GFP-Lifeact and GFP-FABD2 showed similar changes in actin density and paralellness in response to ER structure-modifying protein over-expression and almost no significant changes in bundling were seen with GFP-Lifeact-or GFP-FABD2-marked actin cytoskeleton compared to the control condition (Figures S2 and S3, Tables S5 and S6).

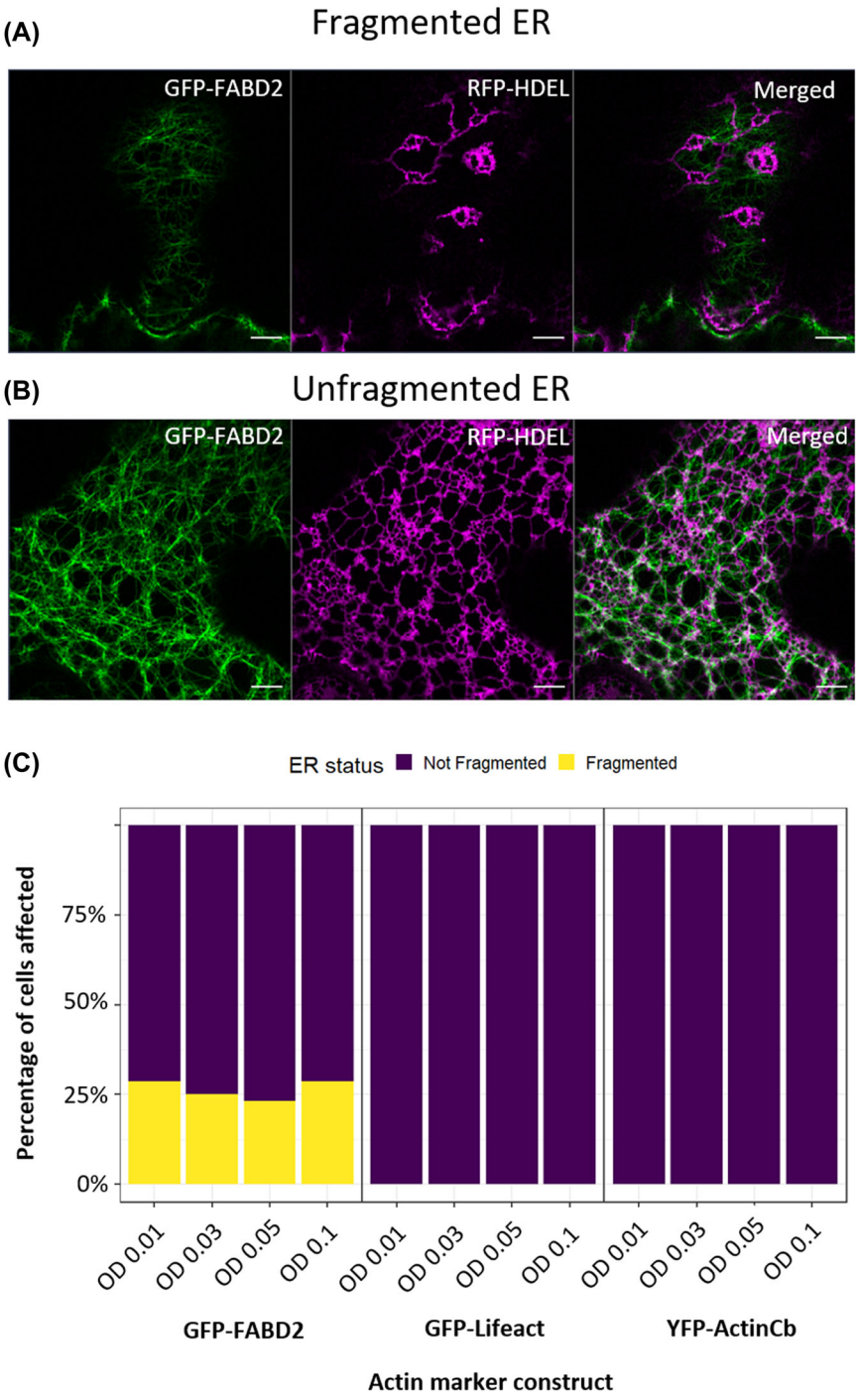


**FIGURE 3** Transient over-expression of GFP-FABD2 can cause fragmentation of the ER, irrespective of the optical density of the infiltration medium. Transient expression of GFP-FABD2 (green) and the ER marker RFP-HDEL (magenta) showing (A) and ER fragmentation phenotype and (B) unfragmented ER, (C) a graph comparing the occurrence of ER fragmentation with various actin markers, GFP-FABD2, GFP-Lifeact and YFP-ActinCb. Scale bars = 5 $\mu$m. Results taken from three biological repeats, with 78 technical repeats

## 3 | DISCUSSION

### 3.1 | Labelling of the actin cytoskeleton can impact on ER structure and dynamics

Here we have shown that labelling of the actin cytoskeleton with fluorescent markers can impact on ER structure and remodelling. FABD2 also changed the structure of the ER most significantly both in transient expression on tobacco epidermal leaf cells as well as in stable expression in Arabidopsis. There have been variable reports on the effect of FABD2 and Lifeact on plant development and normal cellular functioning, with an early study suggesting no significant difference in the overall development and root length of Arabidopsis plants stably expressing FABD2 and Lifeact.[63] However, a more recent, nuanced study into the effect of actin marker expression levels on pollen tube growth has shown that high levels of FABD2 over-expression have severe effects on the rate of pollen tube growth, with Lifeact over-expression having

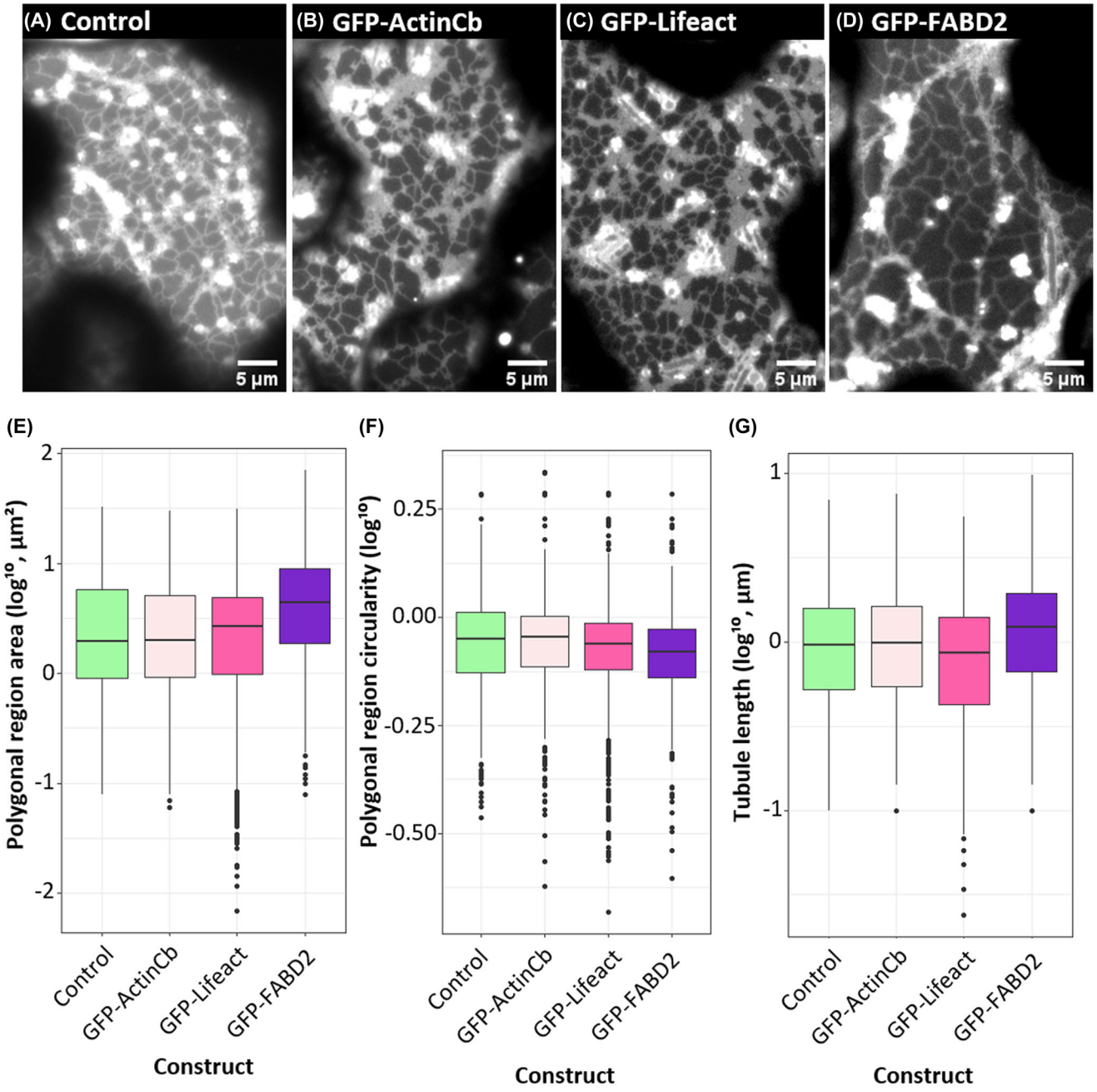


**FIGURE 4** Stable expression of GFP-FABD2 affects the structure of the ER. The ER of 7 day old Arabidopsis leaf epidermal cells stably stained using Rhodamine B hexyl ester in a control Col-0 plant (A) and in Arabidopsis stably expressing (B) GFP-ActinCb, (C) GFP-Lifeat and (D) GFP-FABD2. (E) The mean polygonal region area that is entirely enclosed by the ER displayed as a series of boxplots. The upper whisker extends to the largest value no further than 1.5 times the upper hinge (75% quantile), while the lower whisker extends to the smallest value greater than 1.5 times the lower hinge (25% quantile). Results are shown for three biological repeats, for control, $n = 8$; GFP-ActinCb $n = 5$; GFP-Lifeact, $n = 8$; GFP-FABD2, $n = 8$ cells. *** denotes a significant difference in distribution calculated using Kruskal-Wallis, $p$-value < 0.01, followed by a Tukey's post hoc comparison. Scale bars = 5 $\mu$m

significant, but less severe effects.[73] Here we have found that at commonly used ODs of 0.01 to 0.1, GFP-FABD2 can cause fragmentation of the ER and a reduction in the rate of ER remodelling. This could be due to a reduction in the formation of ER streams that require proper actin orientation and organisation to form.[43] Taken together with recent studies suggesting that FABD2 may perturb pollen tube function, we suggest that FABD2 over-expression might perturb the normal development of actin bundles that play an essential role in cell function.

Previous work by Rocchetti et al.[62] revealed that the meandering index of Golgi bodies is reduced upon

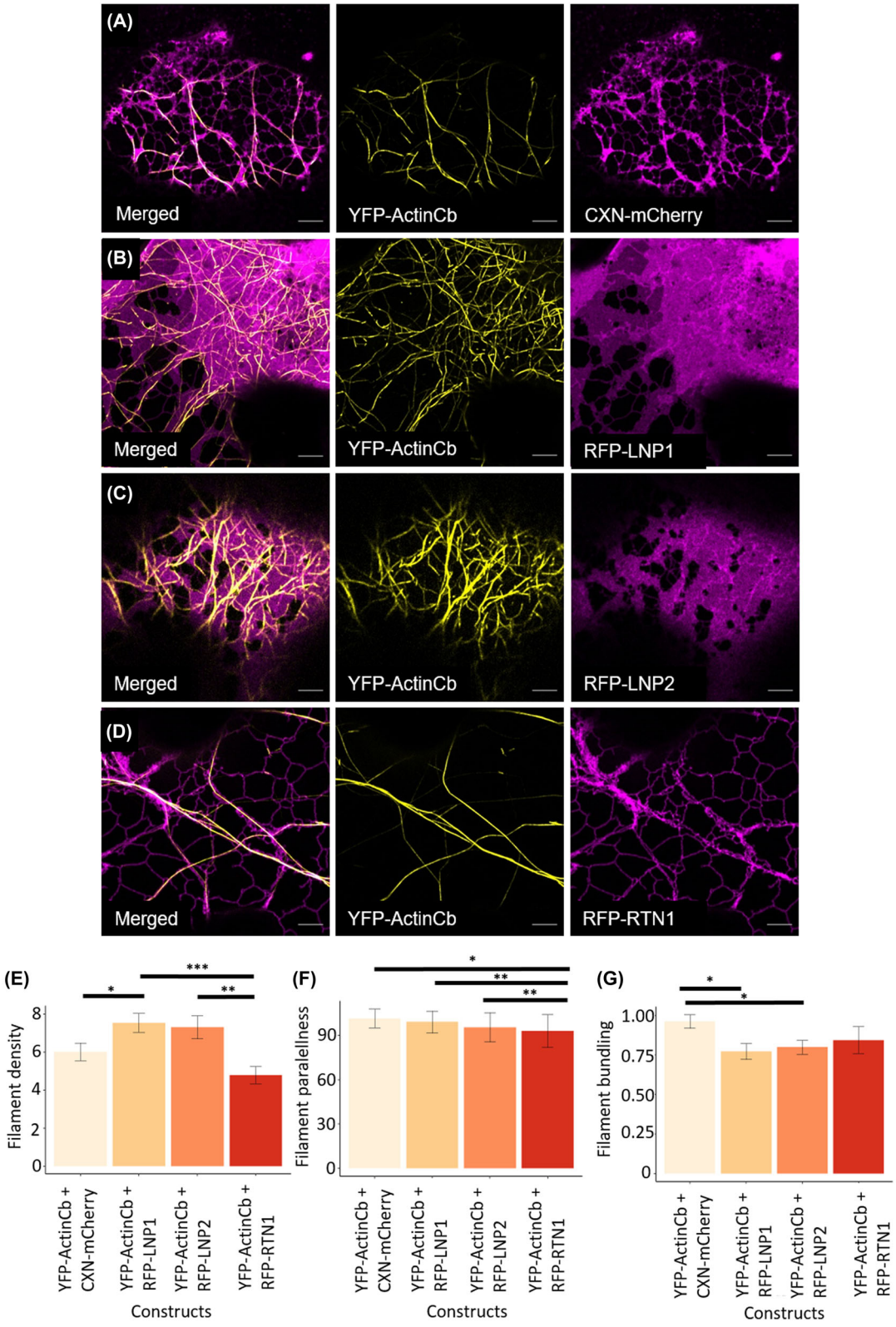


**FIGURE 5** The effect of modified ER structure on the underlying actin cytoskeleton. Merged and single images of the actin marker YFP-ActinCb (yellow) and ER membrane proteins (magenta) including (A) CXN-mCherry, (B) RFP-LNP1 which induces cisternae, (C) RFP-LNP2 which induces cisternae and (D) RFP-RTN1 which produces tubules. Comparison of three actin architecture metrics measured using the 'LPX' plugins. These include (E) actin filament density, (F) actin filament paralellness and (G) actin filament bundling. Significant differences are denoted with asterisk, where **p*-value ≤ 0.05; ***p*-value ≤ 0.01; ****p*-value ≤ 0.001. Results shown from 4 biological replicas and multiple technical replicas (CXN-mCherry, $n = 38$; RFP-LNP1, $n = 34$; RFP-LNP2, $n = 28$; RFP-RTN1, $n = 21$)

**TABLE 2** Mean percentage change in measured ER structure metrics in Arabidopsis lines stably expressing actin markers

| ER structural subdomain | Variable | GFP-ActinCb | GFP-Lifeact | GFP-FABD2 |
|---|---|---|---|---|
| **Tubules** | Length | +2.6% | −12.5% | +25.0% |
| **Polygonal region** | Area | −4.5% | −11.4% | +61.5% |
| | Circularity | +1.3% | −2.4% | −6.1%* |
| | Roughness | −1.5% | +1.2% | +5.8%* |

*Note*: The mean percentage change in ER structure metrics measured in Arabidopsis lines stably expressing GFP-ActinCb, GFP-Lifeact and GFP-FABD2. Comparisons are all given against the control ER structure. Only ER metrics that show a significant change after ANOVA analysis (Table S3) are included. Significant changes in the in ER structure and dynamics after applying a post hoc Tukey's HSD (with Bonferroni correction applied to all *p*-values) are denoted using asterisks. Results are shown for three biological repeats, for control, $n = 8$; GFP-ActinCb $n = 5$; GFP-Lifeact, $n = 8$; GFP-FABD2, $n = 8$ cells.

expression of GFP-Lifeact, suggesting more unidirectional movement of Golgi bodies, whereas expression of ActinCb reduces the speed of Golgi movement. Here all tested markers also affect the distribution of Golgi bodies most likely due to effects on ER dynamics. The effect is similar to Golgi body distribution observed after Lat B treatment[41] providing further evidence that actin labelling impacts ER structure/dynamics as well as the distribution and dynamics of the Golgi bodies.

### 3.2 | The structure of the ER and underlying actin architecture are interlinked

It has been known for some time that the architecture of the actin cytoskeleton and the structure and dynamics of the plant ER vary between cell type and developmental stage.[72,58,74,42,39] Furthermore, it has been clear that normal functioning and structure of filamentous actin are required to maintain a 'normal' ER structure.[48,50,42,46] Changing the structure of the ER by modifying cytosolic pH has also previously been shown to not affect the underlying actin cytoskeleton.[51] However, our research showed that the over-expression of ER-shaping proteins does impact on the structure of the actin cytoskeleton. ER cisternae appeared to be closely associated with densely packed, fine actin filaments, clearly visible when the proportion and size of cisternae is increased using transient over-expression of both members of the Arabidopsis Lunapark protein family. With over-expression of RTN1, the actin filamentous network appeared sparser, with potentially an increase in actin bundles or simply actin filaments positioned so close together that they are below the resolution limit. This change was not significant in terms of the percentage cell occupancy by visible actin filaments. However, this tendency to form bundles, with large spaces between them, affected the orientation of actin filaments, with the majority of filaments becoming orientated in a similar direction. These results indicated that modifications to the ER structure may also affect the structure of the underlying actin cytoskeleton. It must be noted, however, that the impact of ER-shaping proteins on actin architecture may be through indirect mechanisms, such as through the modification of the dynamics of other organelles, for example the Golgi bodies, which may in turn influence the organisation of the actin cytoskeleton.

## 4 | MATERIALS AND METHODS

### 4.1 | Plant material and transformation

All experiments performed on either 4- to 6-week-old *N. tabacum* grown in greenhouse conditions at 23°C or 7- to 10-day-old Arabidopsis grown on ½ MS plates. Transient transformation of tobacco leaves is performed using agrobacterium-mediated transformation. Transgenic agrobacteria were grown in LB with the necessary selection antibiotics, pelleted by centrifugation (2200 × *g* for 5 min, room temperature) and washed once and resuspended in the infiltration media composed of 5 mg/ml glucose, 50 mM MES, 2 mM Na3PO4 and 1 mM acetosyringone. The bacterial solution is diluted to an appropriate concentration of between $OD_{600}$ 0.1–0.01. The final solution is injected through small punctures in the leaf made by pipette tips using a 1 ml syringe. After infiltration, plants were kept at 23°C for 3–4 days prior to imaging.

Stable transformation of Arabidopsis seedlings for ActinCb and Lunapark proteins was performed as by Clough and Bent.[75] Briefly, pelleted transformed agrobacterium were resuspended in a 5% sucrose, 500 $\mu$l/L Silwet 77 solution. The flowering stems of Arabidopsis were dipped into this media and agitated for 1 min, after which the plant is removed and wrapped in Clingfilm for 24 h to ensure agrobacterium survival and maximum transformation success. Arabidopsis seeds were initially sterilised for 3 min in 70% ethanol, dried at room temperature and then transferred to ½ strength MS plates. After 3 days' stratification

in the dark at 4°C, Arabidopsis seedlings were transferred to an incubator and grown at 21°C for a further 7–10 days.

The following previously published constructs and stable lines were used: 35S::GFP-fimbrin actin-binding domain 2 (GFP-FABD2)[58,59] and 35S::GFP-Lifeact.[60]

## 4.2 | Imaging

Confocal microscopy was performed with a Zeiss LSM880 with an Airyscan detector using a Zeiss PlanApo 100×/1.46 NA oil immersion objective. An excitation wavelength of 488 nm was used to observed GFP, 561 nm for RFP and 514 nm for YFP.

## 4.3 | Latrunculin B treatment

In preparation for drug treatments, approximately 25 $mm^2$ leaf segments are cut from transformed tobacco. These are incubated abaxial side down in 25 $\mu$M Lat B at room temperature for 30 min with the leaf surface in direct contact with the Lat B. To prevent washout affects, the leaf pieces are mounted for imaging in the Lat B solution.

## 4.4 | Rhodamine B staining

Rhodamine B hexyl ester was used to stain the ER in Arabidopsis seedlings stably expressing the relevant actin markers. Arabidopsis seedlings were transferred to a 1 $\mu$M Rhodamine B hexyl ester solution and were incubated for 15 min at room temperature. After incubation, the seedling is washed briefly in distilled water a mounted on a glass slide in preparation for imaging.

## 4.5 | Image analysis

### 4.5.1 | Golgi body distribution

Golgi body distribution was assessed as in Renka[77] and Vieira et al.[76] Briefly, images of Golgi body distribution were collected and cropped to the largest possible rectangle containing only cell area within the field of view. Using the ImageJ multi-point tool, the co-ordinates of each Golgi body were manually obtained. The distance between Golgi was calculated in R using the Tripack package.[77]

### 4.5.2 | ER structure and dynamics

The structure and dynamics of the ER was performed as described in Pain et al.[41] using the AnalyzER software. In brief, time-series of confocal images are imported, background subtracted and up sampled to prevent downstream pixilation errors. Cisternae are segmented using an opening function and are subsequently mapped back onto the underlying image by active contouring. The tubular network is segmented using phase congruency enhancement and then reduced to a single pixel wide skeleton running down the centre of each tubule. Polygonal regions are defined as regions of cytoplasm fully enclosed by the ER and are segmented by taking the negative network of the tubular skeleton and cisternae. Several measures of ER structure are produced at this stage, including tubule length, cisternae size and geometry (elongation and roughness), polygonal region size and geometry. The movement of the ER is identified using the Farnebäck method, which identified both fine and coarse remodelling of the ER using a three-level image pyramid. A neighbourhood of 5 pixels is used for initial detection. This provides a measure of the movement of the ER, is subcategorised by ER morphological feature (either cisternae or tubules) and is calculated as a global value (vector sum of speeds for each pixel in the image) or a maximum speed, the maximum speed of any pixel in the time-series. However, this measure does not well capture the proportion of the ER that remains stationary for an extended period of time, in particular ER-plasma membrane contact sites. For analysis of the dynamic behaviour of stable regions of the ER, an additional measure, network persistency, is also calculated. The persistency of the ER is calculated by dilating the images of the ER skeleton and cisternae by the user define half of the full width half minimum width of tubules within the image. These binary images are summed over a defined period of 12.5 s to provide a measure of the persistency of each component of the ER in seconds.

Cisternae texture metrics (cisternae contrast, correlation, energy and homogeneity) use texture based analysis to identify subresolution modifications in the distribution of fluorescent lumenal markers through cisternae. Once the cisternae have been identified as described above, the intensity value of each pixel in a cisternae is compared to the intensity of surrounding pixels to give a grey-level co-occurrence matrix (GLCM). Several measurements that describe the GLCM and summarise the texture information contained within each cisternae are calculated. Full details are provided in Table S1.

Statistical analysis of ER structure and dynamic changes was performed using the designated statistical analysis package that was produced to accompany AnalyzER. A MANOVA is performed first to identify whether there are significant changes in ER structure and dynamics between the treatment groups. Where a statistically significant difference is identified, further analysis by ANOVAs is used with a Tukey's HSD post hoc analysis to identify which variables differ between groups. A Bonferroni correction is applied at this stage to correct for multiple comparisons.

### 4.5.3 | Quantifying actin structure

Actin structure was quantified using the LPX ImageJ plugin as described in.[78] Briefly, an ROI for each cell was created using the 'Freehand' selections tool. The area and angle of the long cell axis of the cell was measured using the ROI. Any area outside of the region of interest is masked. Finally, the actin network was skeletonised using the following parameters: giwsiter = 5, mdnmsLen = 20, pickup = otsu, shaveLen = 5 and delLen = 5. These results are processed according to Higaki,[78] specifically ensuring that actin filament density is normalised to cell area calculated from the ROI drawn around the cell in the first step.

## ACKNOWLEDGEMENTS

C.P. has been funded by the Oxford Doctoral Training Program (BBSRC: BB/M011224/1) and a postdoctoral bursary from Oxford Brookes University. F.T has been supported by Leverhulme Trust funding RGP-2015-1927 to V.K. S.W. was funded by an Oxford Brookes University Nigel Groome PhD studentship. V.K. received further funding by a BBSRC Engineering Biology Breakthrough Ideas (BB/W011166/1).

We are grateful to Dr Mike Deeks for the stable Lifeact plants and thank Dr Tijs Ketelaar for the stable FABD2 plants.

## AUTHOR CONTRIBUTIONS

V.K. conceived of the study and wrote the manuscript with contributions from all the authors listed (C.P., F.T., S.W. and P.W.). Experiments were performed by C.P., F.T. and S.W. C.P. analysed the data. V.K. agrees to serve as the author responsible for contact and ensures communication.

## STATEMENT ON DATA SHARING

Data in this publication is available from the corresponding author upon reasonable request.

## BRIEF SUMMARY STATEMENT

The expression of common actin markers or endoplasmic reticulum-shaping proteins that influence actin or ER architecture reveals the closely inter-related nature of the actin cytoskeleton and the ER.

## ORCID

*Pengwei Wang* https://orcid.org/0000-0001-8882-3447
*Verena Kriechbaumer* https://orcid.org/0000-0003-3782-5834

## REFERENCES

1. Jan, C. H., Williams, C. C., & Weissman, J. S. (2014). Principles of ER cotranslational translocation revealed by proximity-specific ribosome profiling. *Science*, *346*(6210), 1257521.
2. Eichmann, R., & Schäfer, P. (2012). The endoplasmic reticulum in plant immunity and cell death. *Frontiers in Plant Science*, *3*, 200.
3. Chen, Y. F., Randlett, M. D., Findell, J. L., & Schaller, G. E. (2002). Localization of the ethylene receptor ETR1 to the endoplasmic reticulum of Arabidopsis. *Journal of Biological Chemistry*, *277*(22), 19861–19866.
4. Friml, J., & Jones, A. R. (2010). Endoplasmic reticulum: The rising compartment in auxin biology. *Plant Physiology*, *154*(2), 458–462.
5. Hawes, C., Kiviniemi, P., & Kriechbaumer, V. (2015). The endoplasmic reticulum: A dynamic and well-connected organelle. *Journal of Integrative Plant Biology*, *57*(1), 50–62.
6. Zhang, C., Mallery, E., Reagan, S., Boyko, V. P., Kotchoni, S. O., & Szymanski, D. B. (2013). The endoplasmic reticulum is a reservoir for WAVE/SCAR regulatory complex signaling in the Arabidopsis leaf. *Plant Physiology*, *162*(2), 689–706.
7. Resentini, F., Ruberti, C., Grenzi, M., Bonza, M. C., & Costa, A. (2021). The signatures of organellar calcium. *Plant Physiology*, *187*(4), 1985–2004.
8. Galili, G. (2004). ER-derived compartments are formed by highly regulated processes and have special functions in plants. *Plant Physiology*, *136*(3), 3411–3413.
9. Winder, S. J., & Ayscough, K. R. (2005). Actin-binding proteins. *Journal of Cell Science*, *118*(Pt 4), 651–654.
10. Uribe, R., & Jay, D. (2009). A review of actin binding proteins: New perspectives. *Molecular Biology Reports*, *36*(1), 121–125.
11. Barrero, R. A., Umeda, M., Yamamura, S., & Uchimiya, H. (2002). Arabidopsis cap regulates the actin cytoskeleton necessary for plant cell elongation and division. *Plant Cell*, *14*(1), 149–163.
12. Robertson, A. S., Smythe, E., & Ayscough, K. R. (2009). Functions of actin in endocytosis. *Cellular and Molecular Life Sciences*, *66*(13), 2049–2065.
13. Johnson, J. L., Monfregola, J., Napolitano, G., Kiosses, W. B., & Catz, S. D. (2012). Vesicular trafficking through cortical actin during exocytosis is regulated by the Rab27a effector JFC1/Slp1 and the RhoA-GTPase-activating protein Gem-interacting protein. *Molecular Biology of the Cell*, *23*(10), 1902–1916.
14. Mooren, O. L., Galletta, B. J., & Cooper, J. A. (2012). Roles for actin assembly in endocytosis. *Annual Review of Biochemistry*, *81*, 661–686.
15. Wang, P., & Hussey, P. J. (2015). Interactions between plant endomembrane systems and the actin cytoskeleton. *Frontiers in Plant Science*, *6*, 422.
16. Tian, M., Chaudhry, F., Ruzicka, D. R., Meagher, R. B., Staiger, C. J., & Day, B. (2009). Arabidopsis actin-depolymerizing factor AtADF4 mediates defense signal transduction triggered by the *Pseudomonas syringae* effector AvrPphB. *Plant Physiology*, *150*(2), 815–824.
17. Day, B., Henty, J. L., Porter, K. J., & Staiger, C. J. (2011). The pathogen-actin connection: A platform for defense signaling in plants. *Annual Review of Phytopathology*, *49*, 483–506.
18. Henty-Ridilla, J. L., Shimono, M., Li, J., Chang, J. H., Day, B., & Staiger, C. J. (2013). The plant actin cytoskeleton responds to signals from microbe-associated molecular patterns. *PLoS Pathogens*, *9*(4), e1003290.
19. Lin, C., Lemarchand, L., Euler, R., & Sparkes, I. (2018). Modeling the geometry and dynamics of the endoplasmic reticulum network. *IEEE/ACM Transactions on Computational Biology and Bioinformatics*, *15*(2), 377–386.

20. Stephenson, J., & Hawes, C. (1986). Stereology and stereometry of endoplasmic reticulum during differentiation in the maize root cap. *Protoplasma*, *131*, 32–46.
21. Shibata, Y., Voeltz, G. K., & Rapoport, T. A. (2006). Rough sheets and smooth tubules. *Cell*, *126*(3), 435–439.
22. Terasaki, M., Shemesh, T., Kasthuri, N., Klemm, R. W., Schalek, R., Hayworth, K. J., Hand, A. R., Yankova, M., Huber, G., Lichtman, J. W., Rapoport, T. A., & Kozlov, M. M. (2013). Stacked endoplasmic reticulum sheets are connected by helicoidal membrane motifs. *Cell*, *154*(2), 285–296.
23. Sparkes, I., Tolley, N., Aller, I., Svozil, J., Osterrieder, A., Botchway, S., Mueller, C., Frigerio, L., & Hawes, C. (2010). Five Arabidopsis reticulon isoforms share endoplasmic reticulum location, topology, and membrane-shaping properties. *Plant Cell*, *22*(4), 1333–1343.
24. Tolley, N., Sparkes, I., Craddock, C. P., Eastmond, P. J., Runions, J., Hawes, C., & Frigerio, L. (2010). Transmembrane domain length is responsible for the ability of a plant reticulon to shape endoplasmic reticulum tubules *in vivo*. *Plant Journal*, *64*(3), 411–418.
25. Kriechbaumer, V., Botchway, S. W., Slade, S. E., Knox, K., Frigerio, L., Oparka, K., & Hawes, C. (2015). Reticulomics: Protein-protein interaction studies with two plasmodesmata-localized reticulon family proteins identify binding partners enriched at plasmodesmata, endoplasmic reticulum, and the plasma membrane. *Plant Physiology*, *169*(3), 1933–1945.
26. Kriechbaumer, V., Breeze, E., Pain, C., Tolmie, F., Frigerio, L., & Hawes, C. (2018). Arabidopsis Lunapark proteins are involved in ER cisternae formation. *New Phytologist*, *219*(3), 990–1004.
27. Zheng, H., Kunst, L., Hawes, C., & Moore, I. (2004). A GFP-based assay reveals a role for RHD3 in transport between the endoplasmic reticulum and Golgi apparatus. *Plant Journal*, *37*(3), 398–414.
28. Chen, J., Stefano, G., Brandizzi, F., & Zheng, H. (2011). Arabidopsis RHD3 mediates the generation of the tubular ER network and is required for Golgi distribution and motility in plant cells. *Journal of Cell Science*, *124*(Pt 13), 2241–2252.
29. Maneta-Peyret, L., Lai, Y. S., Stefano, G., Fouillen, L., Brandizzi, F., & Moreau, P. (2014). Phospholipid biosynthesis increases in RHD3-defective mutants. *Plant Signaling and Behavior*, *9*(9), e29657.
30. Hamada, T., Tominaga, M., Fukaya, T., Nakamura, M., Nakano, A., Watanabe, Y., Hashimoto, T., & Baskin, T. I. (2012). RNA processing bodies, peroxisomes, Golgi bodies, mitochondria, and endoplasmic reticulum tubule junctions frequently pause at cortical microtubules. *Plant & Cell Physiology*, *53*(4), 699–708.
31. Hamada, T., Ueda, H., Kawase, T., & Hara-Nishimura, I. (2014). Microtubules contribute to tubule elongation and anchoring of endoplasmic reticulum, resulting in high network complexity in Arabidopsis. *Plant Physiology*, *166*(4), 1869–1876.
32. Griffing, L. R., Lin, C., Perico, C., White, R. R., & Sparkes, I. (2017). Plant ER geometry and dynamics: Biophysical and cytoskeletal control during growth and biotic response. *Protoplasma*, *254*(1), 43–56.
33. Terasaki, M., Chen, L. B., & Fujiwara, K. (1986). Microtubules and the endoplasmic reticulum are highly interdependent structures. *Journal of Cell Biology*, *103*(4), 1557–1568.
34. Schroeder, L. K., Barentine, A. E. S., Merta, H., Schweighofer, S., Zhang, Y., Baddeley, D., Bewersdorf, J., & Bahmanyar, S. (2019). Dynamic nanoscale morphology of the ER surveyed by STED microscopy. *Journal of Cell Biology*, *218*(1), 83–96.
35. Smith, L. G., & Oppenheimer, D. G. (2005). Spatial control of cell expansion by the plant cytoskeleton. *Annual Review of Cell and Developmental Biology*, *21*, 271–295.
36. Le, J., Mallery, E. L., Zhang, C., Brankle, S., & Szymanski, D. B. (2006). Arabidopsis BRICK1/HSPC300 is an essential WAVE-complex subunit that selectively stabilizes the Arp2/3 activator SCAR2. *Current Biology*, *16*(9), 895–901.
37. Fu, Y. (2015). The cytoskeleton in the pollen tube. *Current Opinion in Plant Biology*, *28*, 111–119.
38. Zhang, H. M., Colyvas, K., Patrick, J. W., & Offler, C. E. (2017). A $Ca^{2+}$-dependent remodelled actin network directs vesicle trafficking to build wall ingrowth papillae in transfer cells. *Journal of Experimental Botany*, *68*(17), 4749–4764.
39. Ridge, R. W., Uozumi, Y., Plazinski, J., Hurley, U. A., & Williamson, R. E. (1999). Developmental transitions and dynamics of the cortical ER of Arabidopsis cells seen with green fluorescent protein. *Plant & Cell Physiology*, *40*(12), 1253–1261.
40. Sparkes, I., Runions, J., Hawes, C., & Griffing, L. (2009). Movement and remodeling of the endoplasmic reticulum in nondividing cells of tobacco leaves. *Plant Cell*, *21*(12), 3937–3949.
41. Pain, C., Kriechbaumer, V., Kittelmann, M., Hawes, C., & Fricker, M. (2019). Quantitative analysis of plant ER architecture and dynamics. *Nature Communication*, *10*(1), 984.
42. Pain, C., & Kriechbaumer, V. (2020). Defining the dance: Quantification and classification of endoplasmic reticulum dynamics. *Journal of Experimental Botany*, *71*(6), 1757–1762.
43. Ueda, H., Yokota, E., Kutsuna, N., Shimada, T., Tamura, K., Shimmen, T., Hasezawa, S., Dolja, V. V., & Hara-Nishimura, I. (2010). Myosin-dependent endoplasmic reticulum motility and F-actin organization in plant cells. *PNAS*, *107*(15), 6894–6899.
44. Cao, P., Renna, L., Stefano, G., & Brandizzi, F. (2016). SYP73 anchors the ER to the actin cytoskeleton for maintenance of ER integrity and streaming in Arabidopsis. *Current Biology*, *26*(23), 3245–3254.
45. Wang, P., & Hussey, P. J. (2017). Networked 3B: A novel protein in the actin cytoskeleton-endoplasmic reticulum interaction. *Journal of Experimental Botany*, *68*(7), 1441–1450.
46. Sparkes, I. A., Teanby, N. A., & Hawes, C. (2008). Truncated myosin XI tail fusions inhibit peroxisome, Golgi, and mitochondrial movement in tobacco leaf epidermal cells: A genetic tool for the next generation. *Journal of Experimental Botany*, *59*(9), 2499–2512.
47. Peremyslov, V. V., Prokhnevsky, A. I., & Dolja, V. V. (2010). Class XI myosins are required for development, cell expansion, and F-actin organization in Arabidopsis. *Plant Cell*, *22*(6), 1883–1897.
48. Griffing, L. R., Gao, H. T., & Sparkes, I. (2014). ER network dynamics are differentially controlled by myosins XI-K. XI-C, XI-E, XI-I, XI-1, and XI-2. *Frontiers in Plant Science*, *5*, 218.
49. Gibbon, B. C., Kovar, D. R., & Staiger, C. J. (1999). Latrunculin B has different effects on pollen germination and tube growth. *Plant Cell*, *11*(12), 2349–2363.
50. Lin, C., White, R. R., Sparkes, I., & Ashwin, P. (2017). Modeling endoplasmic reticulum network maintenance in a plant cell. *Biophysical Journal*, *113*(1), 214–222.
51. Quader, H., & Fast, H. (1990). Influence of cytosolic pH changes on the organisation of the endoplasmic reticulum in epidermal cells of onion bulb scales: Acidification by loading with weak organic acids. *Protoplasma*, *157*, 216–224.
52. Quader, H., & Liebe, S. (1995). Actin filament-independent formation of tubular endoplasmic reticulum in onion epidermis cells. *Plant Physiology*, *145*, 71–77.

53. Boevink, P., Oparka, K., Santa Cruz, S., Martin, B., Betteridge, A., & Hawes, C. (1998). Stacks on tracks: The plant Golgi apparatus traffics on an actin/ER network. *Plant Journal*, *15*(3), 441–447.
54. Nebenführ, A., Gallagher, L. A., Dunahay, T. G., Frohlick, J. A., Mazurkiewicz, A. M., Meehl, J. B., & Staehelin, L. A. (1999). Stop-and-go movements of plant Golgi stacks are mediated by the acto-myosin system. *Plant Physiology*, *121*(4), 1127–1142.
55. Andersland, J., & Parthasarathy, M. (1993). Conditions affecting depolymerization of actin in plant homogenates. *Journal of Cell Science*, *104*, 1273–1277.
56. Melak, M., Plessner, M., & Grosse, R. (2017). Actin visualization at a glance. *Journal of Cell Science*, *130*(3), 525–530.
57. Kovar, D. R., Staiger, C. J., Weaver, E. A., & McCurdy, D. W. (2000). AtFim1 is an actin filament crosslinking protein from *Arabidopsis thaliana*. *Plant Journal*, *24*(5), 625–636.
58. Ketelaar, T., Anthony, R. G., & Hussey, P. J. (2004). Green fluorescent protein-mTalin causes defects in actin organization and cell expansion in Arabidopsis and inhibits actin depolymerizing factor's actin depolymerizing activity *in vitro*. *Plant Physiology*, *136*(4), 3990–3998.
59. Sheahan, M. B., Rose, R. J., & McCurdy, D. W. (2004). Organelle inheritance in plant cell division: The actin cytoskeleton is required for unbiased inheritance of chloroplasts, mitochondria and endoplasmic reticulum in dividing protoplasts. *Plant Journal*, *37*(3), 379–390.
60. Riedl, J., Crevenna, A. H., Kessenbrock, K., Yu, J. H., Neukirchen, D., Bista, M., Bradke, F., Jenne, D., Holak, T. A., Werb, Z., Sixt, M., & Wedlich-Soldner, R. (2008). Lifeact: A versatile marker to visualize F-actin. *Nature Methods*, *5*(7), 605–607.
61. Smertenko, A. P., Deeks, M. J., & Hussey, P. J. (2010). Strategies of actin reorganisation in plant cells. *Journal of Cell Science*, *123*(Pt 17), 3019–3028.
62. Rocchetti, A., Hawes, C., & Kriechbaumer, V. (2014). Fluorescent labelling of the actin cytoskeleton in plants using a cameloid antibody. *Plant Methods*, *10*, 12.
63. van der Honing, H. S., van Bezouwen, L. S., Emons, A. M., & Ketelaar, T. (2011). High expression of Lifeact in *Arabidopsis thaliana* reduces dynamic reorganization of actin filaments but does not affect plant development. *Cytoskeleton (Hoboken)*, *68*(10), 578–587.
64. Sonobe, S., & Shibaoka, H. (1989). Cortical fine actin filaments in higher plant cells visualized by rhodamine-phalloidin after pretreatment with m-maleimidobenzoyl N-hydroxysuccinimide ester. *Protoplasma*, *148*, 80–86.
65. Takemoto, D., Jones, D. A., & Hardham, A. R. (2003). GFP-tagging of cell components reveals the dynamics of subcellular re-organization in response to infection of Arabidopsis by oomycete pathogens. *Plant Journal*, *33*(4), 775–792.
66. Hardham, A. R., Takemoto, D., & White, R. G. (2008). Rapid and dynamic subcellular reorganization following mechanical stimulation of Arabidopsis epidermal cells mimics responses to fungal and oomycete attack. *Bmc Plant Biology*, *8*, 63.
67. Rodríguez-Serrano, M., Romero-Puertas, M. C., Pazmiño, D. M., Testillano, P. S., Risueño, M. C., Del Río, L. A., & Sandalio, L. M. (2009). Cellular response of pea plants to cadmium toxicity: Cross talk between reactive oxygen species, nitric oxide, and calcium. *Plant Physiology*, *150*(1), 229–243.
68. Avisar, D., Prokhnevsky, A. I., Makarova, K. S., Koonin, E. V., & Dolja, V. V. (2008). Myosin XI-K is required for rapid trafficking of Golgi stacks, peroxisomes, and mitochondria in leaf cells of *Nicotiana benthamiana*. *Plant Physiology*, *146*(3), 1098–1108.
69. Corso, M., Doccula, F. G., de Melo, J. R. F., Costa, A., & Verbruggen, N. (2018). Endoplasmic reticulum-localized CCX2 is required for osmotolerance by regulating ER and cytosolic $Ca^{2+}$ dynamics in Arabidopsis. *PNAS*, *115*(15), 3966–3971.
70. Zapotoczny, B., Braet, F., Kus, E., Ginda-Mäkelä, K., Klejevskaja, B., Campagna, R., Chlopicki, S., & Szymonski, M. (2019). Actin-spectrin scaffold supports open fenestrae in liver sinusoidal endothelial cells. *Traffic (Copenhagen, Denmark)*, *20*(12), 932–942.
71. Nixon-Abell, J., Obara, C. J., Weigel, A. V., Li, D., Legant, W. R., Xu, C. S., Pasolli, H. A., Harvey, K., Hess, H. F., Betzig, E., Blackstone, C., & Lippincott-Schwartz, J. (2016). Increased spatiotemporal resolution reveals highly dynamic dense tubular matrices in the peripheral ER. *Science*, *354*(6311), aaf3928.
72. Ilgenfritz, H., Bouyer, D., Schnittger, A., Mathur, J., Kirik, V., Schwab, B., & Hülskamp, M. (2003). The Arabidopsis stichel gene is a regulator of trichome branch number and encodes a novel protein. *Plant Physiology*, *131*(2), 643–655.
73. Montes-Rodriguez, A., & Kost, B. (2017). Direct comparison of the performance of commonly employed *in vivo* F-actin markers (Lifeact-YFP, YFP-mTn and YFP-FABD2) in tobacco pollen tubes. *Frontiers in Plant Science*, *8*, 1349.
74. Mathur, J., Spielhofer, P., Kost, B., & Chua, N. (1999). The actin cytoskeleton is required to elaborate and maintain spatial patterning during trichome cell morphogenesis in *Arabidopsis thaliana*. *Development (Cambridge, England)*, *126*(24), 5559–5568.
75. Clough, S. J., & Bent, A. F. (1998). Floral dip: A simplified method for agrobacterium-mediated transformation of *Arabidopsis thaliana*. *Plant Journal*, *16*(6), 735–743.
76. Vieira, V., Pain, C., Wojcik, S., Rossi, T. S., Denecke, J., Osterrieder, A., & Kriechbaumer, V. (2020). Living on the edge: The role of Atgolgin-84a at the plant ER-Golgi interface. *Journal of Microscopy*, *280*(2), 158–173.
77. Renka, R. (1996). Algorithm 751: Tripack: A constrained two-dimensional delaunay triangulation package. *ACM Transactions on Mathematical Software*, *22*, 1–8.
78. Higaki, T. (2017). Quantitative evaluation of cytoskeletal organizations by microscopic image analysis. *Plant Morphology*, *29*, 15–21.


## SUPPORTING INFORMATION

Additional supporting information can be found online in the Supporting Information section at the end of this article.

**How to cite this article:** Pain, C., Tolmie, F., Wojcik, S., Wang, P., & Kriechbaumer, V. (2023). intER-ACTINg: The structure and dynamics of ER and actin are interlinked. *Journal of Microscopy*, *291,* 105–118. https://doi.org/10.1111/jmi.13139